Spin Coating of Thin and Ultrathin Polymer Films

DAVID B. HALL,[1,2] PATRICK UNDERHILL,[2]
and JOHN M. TORKELSON[1,2,3]

[1] *Department of Chemical Engineering*
[2] *Materials Research Center*
[3] *Department of Materials Science and Engineering*
Northwestern University
Evanston, Illinois 60208-3120

The spin coating of thin (> 200 nm thick) and ultrathin (< 200 nm thick) polymer films is examined in several solvents of varying volatility over a broad range of polymer solution concentrations and spin speeds. Experimentally measured film thicknesses are compared with a simple model proposed by Bornside, Macosko, and Scriven, which predicts film thickness based on the initial properties of the polymer solution, solvent, and spin speed. This model is found to predict film thickness values within 10% over the entire range of conditions explored, which gave film thicknesses from 10 nm to 33 μm. The model underpredicts film thickness for cases in which a very volatile solvent is used or the initial concentration of polymer is high, while overpredicting film thickness for cases in which a low volatility solvent is used or the initial polymer concentration is very low. These deviations are a consequence of how the model decouples fluid flow and solvent evaporation.

INTRODUCTION

Spin coating from dilute solution is a common method to produce a thin, uniform polymer film on a planar substrate. It is most often employed in the microelectronics industry for the production of photoresists. Photoresists typically have film thicknesses in the micron range, and thus most experimental and mathematical modeling work has focused on conditions by which films with thicknesses in this range may be produced. Very few studies have critically tested proposed models by examining a wide range of film thicknesses and process conditions. Recently, there has been growing interest in ultrathin polymer films (1), i.e., films with thicknesses less than 200 nm. The spin coating of these ultrathin films still remains largely unexplored. This study experimentally examines the spin coating of polymer films under a wide range of process conditions in which both thin and ultrathin films are produced. The results are then compared with those predicted by a simple model.

SPIN COATING BASICS

In the spin coating process, solution is first deposited on the substrate, and the substrate is then accelerated rapidly to the desired rotation rate. Liquid flows radially, owing to the action of centrifugal force, and the excess is ejected off the edge of the substrate. The film continues to thin slowly until disjoining pressure effects cause the film to reach an equilibrium thickness or until it turns solid-like due to a dramatic rise in viscosity from solvent evaporation. The final thinning of the film is then due solely to solvent evaporation. An excellent description of the basic principles involved in the spin coating process is given in a review by Bornside, Macosko, and Scriven (2).

Mathematically modeling the spin coating process is extremely challenging because of the complex coupling of fluid rheology and solvent evaporation. A simple model first proposed by Meyerhofer (3) has been found to capture much of the essential characteristics of the spin coating process even though it decouples evaporation and flow. The film thinning process is treated as occurring through two distinct stages. In the first stage, film thinning is only due to radial outflow. Solvent evaporation is neglected, and the solution concentration is assumed to stay constant at its initial value. This situation is analogous to the thinning of a Newtonian liquid on a rotating disk first derived by Emslie, Bonner, and Peck (4):

$$\frac{dh}{dt} = -\frac{2\rho\omega^2 h^3}{3\eta_0} \tag{1}$$

where h is film thickness, t is spinning time, ρ is liquid density, ω is spin speed, and η_0 is initial solution viscosity. When the rate of film thinning reaches some specified evaporation rate, E, the film is treated as becoming essentially immobile, and the second stage in which all thinning is due to solvent evaporation is en-

tered. Bornside, Macosko, and Scriven (5) proposed that E may be calculated using a mass transfer expression:

$$E = k(x_1^0 - x_{1\infty}) \tag{2}$$

where k is the mass transfer coefficient, x_1^0 is the initial solvent mass fraction in the coating solution, and $x_{1\infty}$ is the solvent mass fraction that would be in equilibrium with the solvent mass fraction in the gas phase. The mass transfer coefficient, k, is given by the following expression:

$$k = \left(\frac{cD_g}{\nu_g^{1/2}\rho}\right)\left(\frac{p_1^\circ M_1}{RT}\right)\omega^{1/2} \tag{3}$$

where c is a constant that depends on the Schmidt number of the overhead gas phase, D_g is the binary diffusivity of the solvent in the overhead gas phase, ν_g is the kinematic viscosity of the overhead gas phase, p_1^0 is the vapor pressure of the pure solvent at temperature T, M_1 is the solvent molecular weight, and R is the ideal gas constant.

Employing *Eqs 1* and *2*, one can calculate a wet film thickness, h_w, at which the film is supposed to become immobile (5):

$$h_w = \left[\left(\frac{3\eta_0}{2\rho\omega^2}\right)k(x_1^0 - x_{1\infty})\right]^{1/3} \tag{4}$$

Further film thinning is due only to evaporation; therefore, the final film thickness, h_f, is

$$h_f = (1 - x_1^0)h_w \tag{5}$$

This simple model captures the experimentally observed scaling (6) of $h_f \sim \eta_0^{1/3}\omega^{-1/2}$, but has been shown to underpredict film thickness in certain conditions due to the neglecting of solvent evaporation in the initial spin off stage (5). More detailed modeling has been performed that takes into consideration how solvent evaporation affects fluid rheology and vice versa, but these studies involve complex numerical methods and often include parameters which are difficult to estimate (7).

PREVIOUS WORK INVOLVING SPIN COATING ULTRATHIN FILMS

Stange *et al.* (8) studied the morphology of ultrathin polystyrene (PS) films spin coated from toluene onto silicon substrates using atomic force microscopy and ellipsometry. They found that 2 nm was the lower film thickness limit at which a continuous, defect-free PS film could be achieved. This film thickness is an order of magnitude smaller than the radius of gyration of the PS chains employed (~ 25 nm for 20,000,000 molecular weight PS) indicating that the polymer chains adopt a highly extended configuration in the film. Extrand (9) found that the lower film thickness limit for a continuous film can depend on the substrate type and the polymer used. The flow of low molecular weight nonvolatile liquids on spinning disks were studied by Forcada and Mate (10). They found that films with thicknesses between 4 and 25 nm could still be modeled as that of a continuum, Newtonian liquid and followed the theory of Emslie (4). However, the apparent viscosity seemed to be as much as 80% higher than that of the bulk fluid.

The only study concerning the effect of process parameters on the spin coating of ultrathin polymer films was published by Extrand (11). Natural rubber, poly(methyl methacrylate) (PMMA), and PS films ranging in thickness from 0.5 to 170 nm were spun from dilute solution onto silicon wafers. No film thickness dependence was found on the volume of initial solution dispensed or the surface treatment of the silicon wafer. Film thickness measurements were found to be consistent with the following scaling:

$$h_f \propto \left(\frac{\eta_0}{\rho\omega}\right)^{1/2}(1 - x_1^0) \tag{6}$$

The results were quantitatively compared with an expression found by integrating *Eq 1* and assuming that all the solvent flashes off at a certain time, t^*, and that no evaporation takes place before t^* [similar to the assumption of Meyerhofer's model (3)]. Determination of t^* was performed by visual observation. Films were found to be approximately twice as thick as predicted, and the discrepancy was blamed on the erroneous assumption that no evaporation occurs before t^*.

EXPERIMENTAL

PS (GPC: M_n = 80,000; M_w = 200,000) and PMMA (GPC: M_n = 50,000; M_w = 94,000) films were spun from solution onto 5-cm-diameter polished silicon wafers that contained a thin native oxide surface layer. The solvents used were toluene, chloroform, and xylene with polymer concentrations ranging from 0.25 wt% to 30 wt%. The initially stationary wafer was flooded with polymer solution until the entire surface was covered and then accelerated to the desired rotation rate. Acceleration times were less than 2 s and total spin times were 60 s. Spin speeds ranged from 500 to 4500 rpm. Spun films were placed under vacuum at room temperature for a period of at least 12 hours even though this further drying process did not seem to affect the final film thickness. Film thickness measurements were performed using a Tencor P10 profilometer, and the calibration was checked with a 14 nm step height standard from VLSI Standards Incorporated. At least ten thickness measurements were taken per film along the centerline of the wafer. Zero shear viscosities, η_0, of the polymer solutions at 30°C were determined using Ubbelohde glass kinematic viscometers.

RESULTS AND DISCUSSION

PS and PMMA films were spun from toluene solutions with initial solution concentrations ranging from

0.5 wt% to 30 wt% PS and 0.5 wt% to 15 wt% PMMA. Continuous films resulted in all cases with no observable "pinhole" type defects. Films spun from the most dilute solutions tended to be the most uniform, while at the highest concentrations (> 15 wt%) the film surfaces tended to exhibit some degree of waviness. These concentrated polymer solutions may be highly non-Newtonian. Surface waves on a non-Newtonian fluid that is spinning on a disk tend not to damp out as readily as for a Newtonian fluid (2). The greater viscosity of the more concentrated solutions may also hinder the damping of surface waves before the fluid layer becomes immobile. Both of these effects could contribute to the waviness in the thickest films that were spun from the more concentrated solutions. Slight variations in film thickness with radial distance from the center of the wafer were also found for certain films spun from the most concentrated solutions. Films exhibiting this phenomenon were thickest at the center of the wafer with progressively decreasing thickness moving radially away from the center. This is a sign of non-Newtonian shear thinning behavior occurring for films spun from the most concentrated solutions, since the shear rate increases from the center of the wafer to the outside edge. The more dilute polymer solutions should have higher critical shear rates for the onset of shear thinning behavior and thus do not exhibit this effect.

Average film thicknesses as a function of spin speed are shown in *Figs. 1* and *2* for each initial solution concentration. Film thicknesses ranged from 12 nm to 33.2 μm for the PS films and from 10 nm to 3.4 μm for the PMMA films. The solid lines in *Figs. 1* and *2* are film thickness predictions based on *Eqs 3–5*. The parameters used in the model are given in *Table 1*. Measured η_0 values as a function of PS and PMMA concentration are shown in *Fig. 3*. Comparing the slopes of the data in *Figs. 1* and *2* to the slope of the model prediction, we see that the expected $h_f \propto \omega^{-1/2}$ scaling holds within experimental error for all cases. This is consistent with results first reported by Extrand (11) for ultrathin polymer films. At high initial PS and PMMA concentrations (> 10 wt%), which correspond to the thickest films, the model tends to underpredict film thickness. This underprediction is consistent with the fact that the model neglects evaporation in the spin-off stage and the subsequent sharp rise in viscosity that follows. Therefore, film thickness predictions would tend to be lower than the actual values. The degree of underprediction becomes more significant as initial polymer concentration increases because, as pointed out in Ref 5, this is the region where viscosity changes most dramatically with polymer concentration. The assumption of Newtonian flow may

Table 1. Parameters for Predicting h_f Values Given in *Figs. 1* and *2* Using *Eqs 3–5*.

T = 303 K
$x_{1\infty}$ = 0
R = 82.06 atm cm³/mol K
ν_g = 0.1553 cm²/s
c = 0.5474 (from Ref. 5)
ρ = 0.87 g/cm³
M_1 = 92 g/mol
p_1° = 0.029 atm (from Ref. 12)
D_g = 0.086 cm²/s
η_0, see *Fig. 3* for individual values

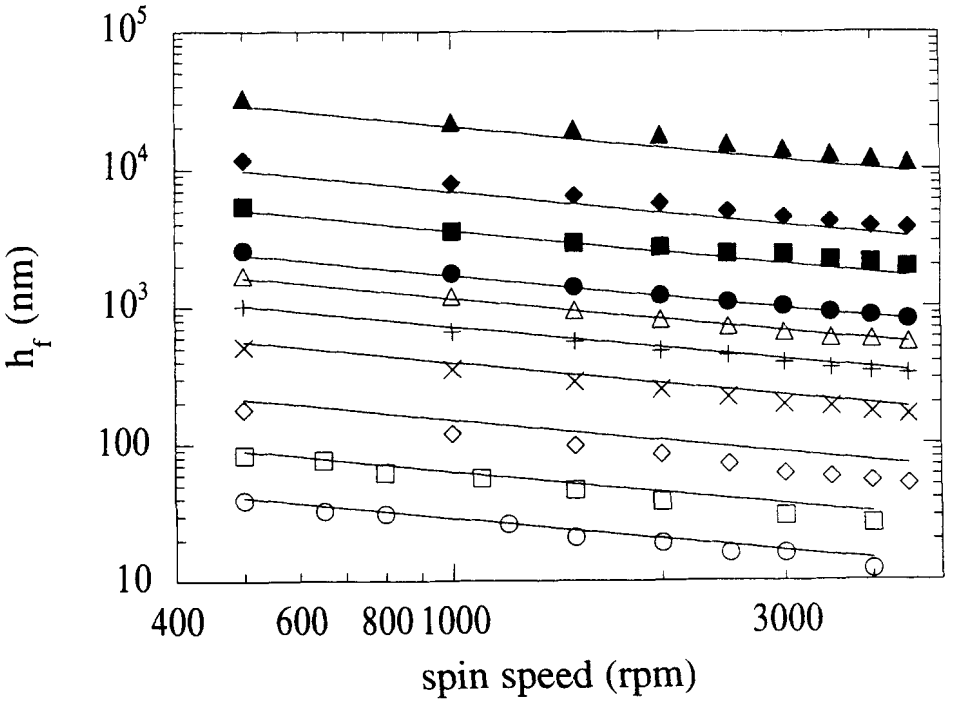

Fig. 1. Film thickness, h_f, as a function of spin speed and initial polymer solution concentration for PS in toluene: (○) 0.5 wt%, (□) 1 wt%, (◇) 2 wt%, (X) 4 wt%, (+) 6 wt%, (Δ) 8 wt%, (●) 10 wt%, (■) 15 wt%, (◆) 20 wt%, and (▲) 30 wt%. Solid lines are predictions of Eq 5 with parameters given in Table 1.

also introduce errors in the predicted film thickness for films spun at high polymer concentration, but they are obviously small compared with those due to neglecting solvent evaporation during spin-off.

At moderate initial PS concentrations (6 wt% to 10 wt%) and for 10 wt% PMMA, the model agrees very well with the experimentally measured h_f values. However, at lower initial concentrations (< 6 wt% for PS and < 10 wt% for PMMA) the model diverges from the data again, this time predicting higher h_f values than actually observed. This effect was not seen in the initial work of Bornside, Macosko, and Scriven (5) who only studied one polymer/solvent system at three different concentrations.

The fact that the model may also overpredict film thickness should not be surprising. One of the key as-

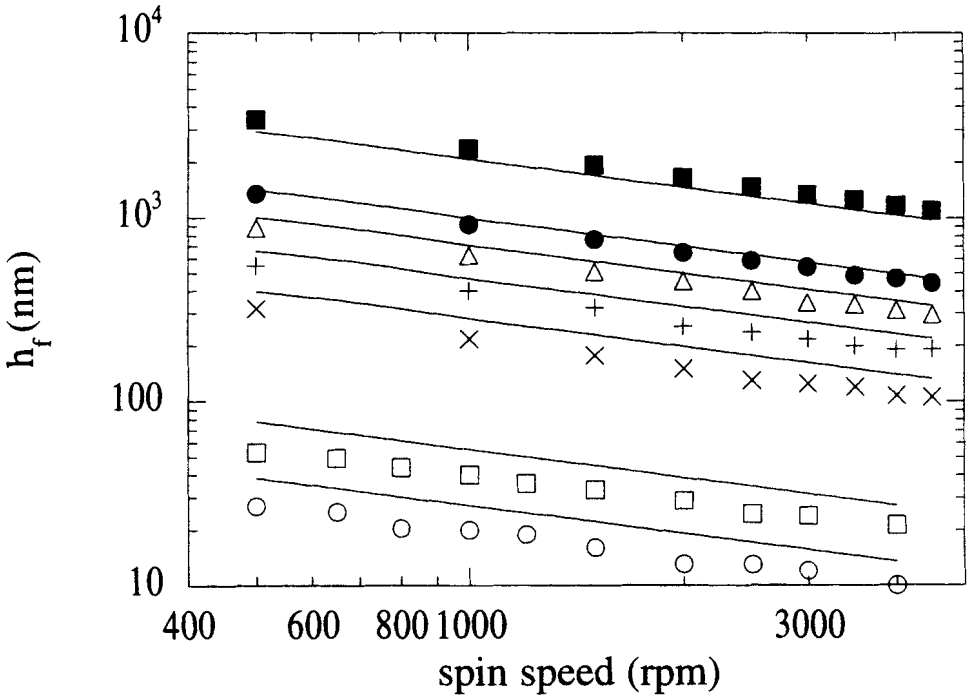

Fig. 2. Film thickness, h_f, as a function of spin speed and initial polymer solution concentration for PMMA in toluene: (○) 0.5 wt%, (□) 1 wt%, (X) 4 wt%, (+) 6 wt%, (Δ) 8 wt%, (●) 10 wt%, and (■) 15 wt% PMMA. Solid lines are predictions of Eq 5 with parameters given in Table 1.

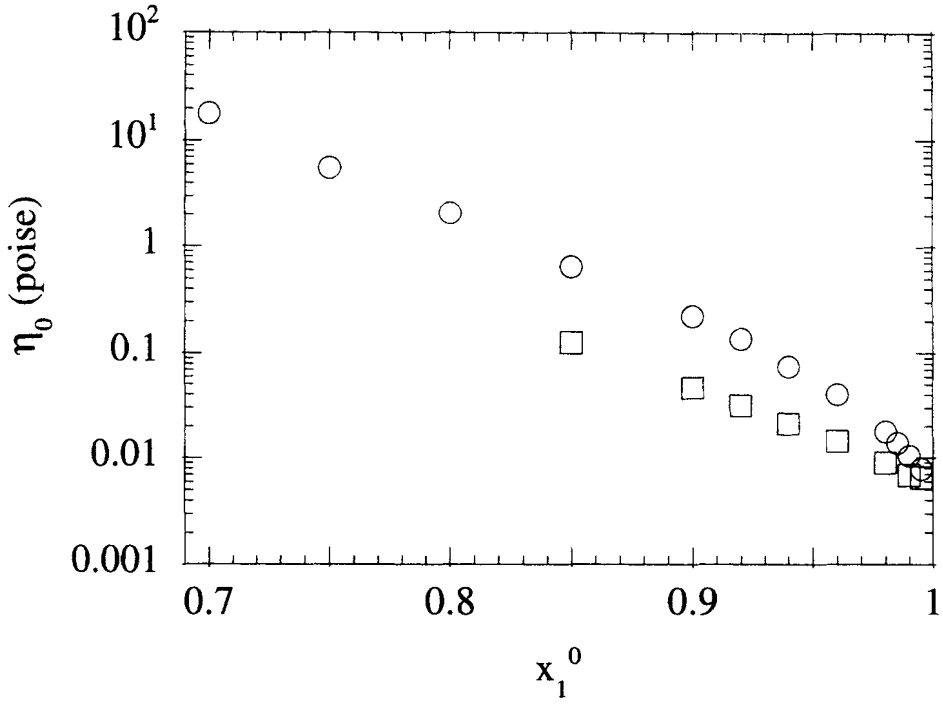

Fig. 3. Initial solution viscosity, η_0, as a function of toluene mass fraction, x_1^0, for (○) PS and (□) PMMA.

Table 2. Parameters for Predicting h_f Values Given in *Figs. 4* and *5* Using *Eqs 3–5*.

chloroform solutions	xylene solutions
ρ = 1.49 g/cm^3	ρ = 0.88 g/cm^3
M_1 = 119.4 g/mol	M_1 = 106.2 g/mol
p_1° = 0.31 atm	p_1° = 0.013 atm
D_g = 0.106 cm^2/s	D_g = 0.074 cm^2/s
T, $x_{1\infty}$, R, v_g, and c: see *Table 1*	T, $x_{1\infty}$, R, v_g, and c: see *Table 1*

sumptions of the model is that all fluid flow halts once the rate of film thinning due to convective outflow, dh/dt in *Eq 1*, reaches a calculated evaporation rate, E, in *Eq 2*. Thus, the model predicts a particular "wet film thickness," h_w, or equivalently, a certain time, t^*_p, when the fluid film becomes immobile, which depends on the initial properties of the polymer solution, solvent volatility, and spin speed. In reality, this is somewhat arbitrary and there is actually a dynamic interplay between evaporation and flow, which may cause the actual time, t^*_a, to be greater or smaller than the predicted t^*_p. For cases in which the model overpredicts h_f, $t^*_a > t^*_p$, there is still flow occurring even though the model predicts that the film is immobile. In dilute solutions, the viscosity may be still low enough to allow significant flow to take place even though the rate of film thinning due to convective outflow may be less than the rate due to evaporation. Underpredictions of h_f are found when $t^*_a < t^*_p$, and quantitative agreement is found when $t^*_a \approx t^*_p$. This assumes that the transition between the flow and evaporation stages is sharp, which appears to be the case for the polymer/solvent conditions employed here, since the slopes of the predicted and experimental curves are equivalent.

Figures 1 and *2* indicate that x_1^0 and η_0 are important in determining how well *Eqs 3–5* quantitatively predict h_f, with low x_1^0 values (high η_0) giving underpredictions of actual h_f and high x_1^0 values (low η_0) giving overpredictions of actual h_f. Another important variable in the calculation of t^*_p is the evaporation rate of the solvent. Highly volatile solvents (large p_1°) evaporate quickly, giving thicker films (also somewhat rougher) and smaller values for t^*_p than less volatile solvents for similar x_1^0 values. *Figure 4* plots h_f as a function of spin speed and initial polymer solution concentration for PS in a highly volatile solvent, chloroform. As expected, h_f values are much larger compared with those films spun from toluene at equivalent initial PS concentrations. Also shown are predictions based on *Eqs 3–5* with parameters given in *Table 2* (η_0 values are not given but showed similar concentration dependencies as found for toluene in *Fig. 3*). In all cases, *Eqs 3–5* underpredict the actual h_f values, indicating that $t^*_a < t^*_p$. In *Fig. 5*, we consider the opposite case in which films are spun from a solvent, xylene, which is less volatile than toluene. For PS in xylene, the model overpredicts the actual h_f values indicating that $t^*_a > t^*_p$.

For a highly volatile solvent such as chloroform, one expects to have very significant evaporation during the spin-off stage, which causes a rapid rise in solution viscosity, thus leading to $t^*_a < t^*_p$ and underpredictions for h_f. However, for a much less volatile sol-

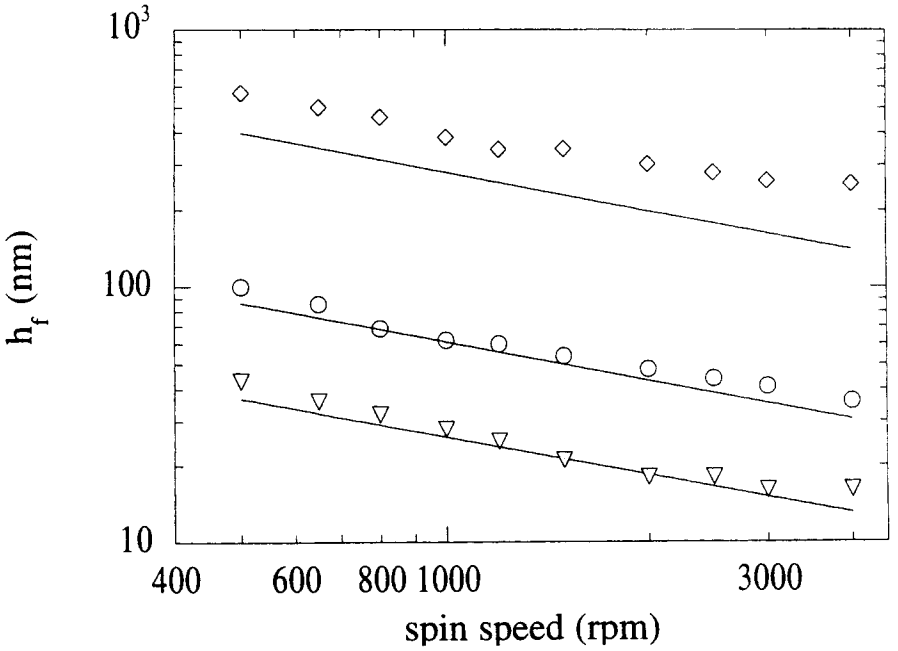

Fig. 4. Film thickness, h_f, as a function of spin speed and initial polymer solution concentration for PS in chloroform: (▽) 0.25 wt% PS, (○) 0.5 wt% PS, and (◇) 2 wt% PS. Solid lines are predictions of Eq 5 with parameters given in Table 2.

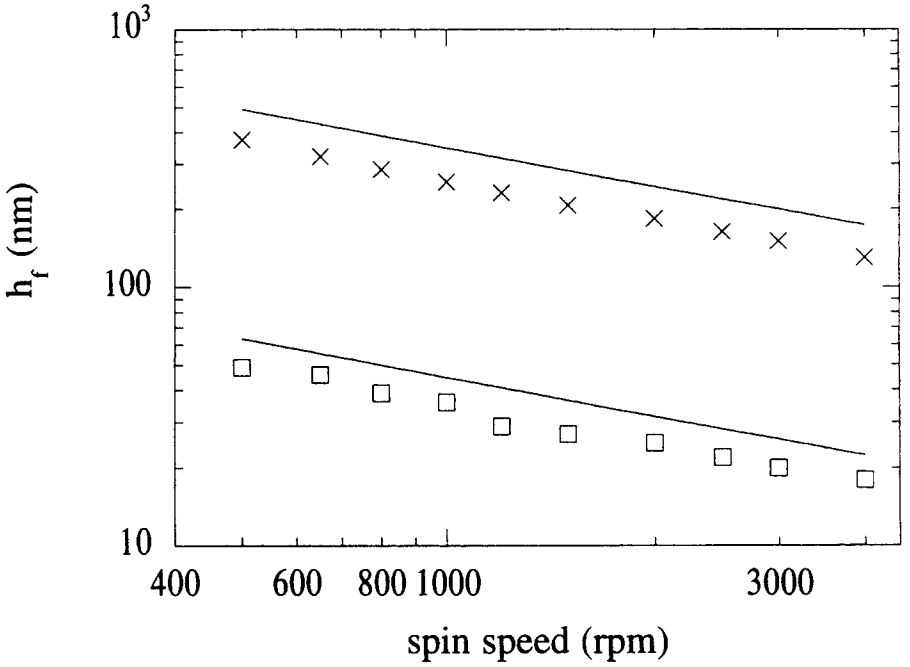

Fig. 5. Film thickness, h_f, as a function of spin speed and initial polymer solution concentration for PS in xylene: (□) 1 wt% PS and (X) 4 wt% PS. Solid lines are predictions of Eq 5 with parameters given in Table 2.

vent such as xylene, one expects evaporation during the spin off stage to be minimal, thus extending the flow time of the fluid film leading to $t^*_a > t^*_p$. Therefore, the volatility of the solvent is also important in determining how well *Eqs 3–5* quantitatively predict h_f.

The results presented here regarding the spin coating of ultrathin polymer films are essentially in agreement with the results first reported by Extrand (11), namely that the $h_f \propto \omega^{-1/2}$ scaling found for thin films still holds. The difference in h_f scaling with η_0 and x_1^0 between *Eqs 3–5* and *Eq 6*, which was used by Extrand for ultrathin films, are difficult to resolve when one examines a narrow range of process conditions and film thicknesses such as those employed in Extrand's study. Our studies show that *Eqs 3–5* predict h_f values surprisingly well over a wide range of conditions. One advantage of using *Eqs 3–5* is that it eliminates the need for experimentally determining t^*.

It is unlikely that significant improvements may be made to the Bornside, Macosko, and Scriven model (5) without resorting to numerical methods. Still, it is quite remarkable that a simple analytical model, which essentially ignores the coupling of solvent evaporation and fluid flow, quantitatively predicts h_f as a function of initial process parameters, usually within 10% of the actual value for thin as well as ultrathin polymer films.

CONCLUSIONS

Spin coating of thin (33.2 μm > h_f > 0.2 μm) and ultrathin (200 nm > h_f > 10 nm) polymer films from dilute solution has been studied as a function of process parameters. Relationships between process parameters and final film thickness found previously for the spin coating of thin films were also found to hold for the spin coating of ultrathin films. Comparisons of measured film thickness to those predicted by a simple analytical model proposed by Bornside, Macosko, and Scriven (5) were found to agree within 10% over the whole film thickness range. The model tends to underpredict film thickness for films spun from solutions with an initially high polymer concentration or solutions in which a highly volatile solvent is used; the model tends to overpredict film thickness for films spun from very dilute solutions or solutions in which a low volatility solvent is used. These deviations from an exact quantitative fit of the experimental data are a consequence of the assumption of the model that fluid flow and evaporation are decoupled.

ACKNOWLEDGMENTS

The authors would like to acknowledge Marianne Husberg for help with several viscosity measurements. This work was supported by the MRL/MRSEC programs of the National Science Foundation (DMR-9632472) at the Northwestern University Materials Research Center.

NOMENCLATURE

c	=	constant that depends on the gas phase Schmidt number.
D_g	=	binary diffusivity of the solvent in the gas.
E	=	evaporation rate.
GPC	=	gel permeation chromatography.
h	=	film thickness.
h_f	=	final film thickness.
h_w	=	wet film thickness at t^*_p.
k	=	mass transfer coefficient.

M_1 = solvent molecular weight.
M_n = number average molecular weight.
M_w = weight average molecular weight.
p_1^o = vapor pressure of solvent.
PS = polystyrene.
PMMA = poly(methyl methacrylate).
R = ideal gas constant.
T = temperature.
t = time.
t^*_a = actual time at which the spin-off stage ends
t^*_p = predicted time at which the spin-off stage ends as defined by *Eq 4*.
x_1^0 = initial solvent mass fraction.
$x_{1\infty}$ = equilibrium solvent mass fraction.
η_0 = initial solution viscosity.
ρ = initial solution density.
ω = spin speed.
ν_g = kinematic viscosity of gas phase.

REFERENCES

1. See, for example, the following: D. B. Hall, J. C. Hooker, and J. M. Torkelson, *Macromolecules*, **30**, 667 (1997); D. B. Hall, R. D. Miller, and J. M. Torkelson, *J. Polym. Sci. B: Polym. Phys.*, **35**, 2795 (1997); J. A. Forrest, K. Dalnoki-Veress, and J. R. Dutcher, *Phys. Rev. E*, **56**, 5705 (1997); J. A. Forrest, K. Dalnoki-Veress, J. R. Stevens, and J. R. Dutcher, *Phys. Rev. Lett.*, **77**, 2002 (1996); B. Frank, A. P. Gast, T. P. Russell, H. R. Brown, and C. Hawker, *Macromolecules*, **29**, 6531 (1996); W. E. Wallace, J. H. van Zanten, and W. L. Wu, *Phys. Rev. E*, **52**, R3329 (1995); J. L. Keddie, R. A. L. Jones, and R. A. Cory, *Faraday Discuss.*, **98**, 219 (1994); G. Reiter, *Macromolecules*, **27**, 3046 (1994).
2. D. E. Bornside, C. W. Macosko, and L. E. Scriven, *J. Imag. Technol.*, **13**, 122 (1987).
3. D. Meyerhofer, *J. Appl. Phys.*, **49**, 3993 (1978).
4. A. G. Emslie, F. T. Bonner, and L. G. Peck, *J. Appl. Phys.*, **29**, 858 (1958).
5. D. E. Bornside, C. W. Macosko, and L. E. Scriven, *J. Electrochem. Soc.*, **138**, 317 (1991).
6. See, for example: J. D. LeRoux and D. R. Paul, *J. Membr. Sci.*, **74**, 233 (1992); L. L. Spangler, J. M. Torkelson, and J. S. Royal, *Polym. Eng. Sci.*, **30**, 644 (1990); B. T. Chen, *Polym. Eng. Sci.*, **23**, 399 (1983); J. H. Lai, *Polym. Eng. Sci.*, **19**, 1117 (1979).
7. See, for example: S. Shimoji, *J. Appl. Phys.*, **66**, 2712 (1989); D. E. Bornside, C. W. Macosko, and L. E. Scriven, *J. Appl. Phys.*, **66**, 5185 (1989); T. Ohara, Y. Matsumoto, and H. Ohasi, *Phys. Fluids A*, **1**, 1949 (1989); R. K. Yonkoski and D. S. Soane, *J. Appl. Phys.*, **72**, 725 (1992).
8. T. G. Stange, R. Mathew, D. F. Evans, and W. A. Hendrickson, *Langmuir*, **8**, 920 (1992).
9. C. W. Extrand, *Langmuir*, **9**, 475 (1993).
10. M. L. Forcada and C. M. Mate, *J. Coll. Int. Sci.*, **160**, 218 (1993); M. L. Forcada and C. M. Mate, *Wear*, **168**, 21 (1993).
11. C. W. Extrand, *Polym. Eng. Sci.*, **34**, 390 (1994).
12. E. R. Gilliland, *Ind. Eng. Chem.*, **26**, 681 (1934).

Received December 1997
Revised April 1998